Russian Chemical Reviews, **51** (10), 1982

961

Translated from *Uspekhi Khimii*, 51 1674 - 1697 (1982)

U.D.C. 547.402:535.34.083.2:538.56

Investigation of Paramagnetic Metallocenes and Diarene Complexes of Transition Metals by Magnetic Resonance Methods

S.P.Solodovnikov

EPR and NMR data for paramagnetic metallocenes and diarene complexes of transition metals are presented. The analysis of the g-factors and the hyperfine and spin-spin interaction constants for the EPR spectra as well as the paramagnetic shifts in the NMR spectra have been used to determine the electronic configurations of the complexes. The manifestation of the Jahn-Teller effect in the EPR spectra of sandwich compounds is described. The scheme of the d-electronic levels in metallocenes and the mechanism of the spin delocalisation are discussed.
The bibliography includes 67 references.

CONTENTS

I. Introduction 961
II. Magnetic properties and the characterisation of the EPR and NMR spectra of paramagnetic sandwich compounds 962
III. NMR spectra of nickelocene 969
IV. EPR spectra of manganocene 970
V. The Jahn-Teller effect in sandwich compounds 970
VI. The electronic structure of metallocenes and the mechanism of spin delocalisation 972

I. INTRODUCTION

The nature of the bond in metallocenes and diarene complexes of metals has continuously attracted the attention of both experimenters and theoreticians. Since 1951, the time of the first synthesis of ferrocene, numerous theoretical studies, which explained the stability and aromaticity of ferrocene, have been carried out. Quantitative comparison of the theoretical results with spectroscopic data serves as an objective test of the reliability of the continuingly improving computational methods.

This review is devoted to the results of the study of paramagnetic sandwich complexes of transition metals. Examination of paramagnetic complexes alone simplifies somewhat the analysis of the electronic structure, since the EPR and NMR parameters are in this case determined by the distribution of one or several unpaired electrons and not all the electrons of the molecule.

Jaffé[1] was the first to point out the unusual nature of the chemical bond in metallocenes, consisting in the fact that this many-electron bond is formed by the molecular π orbitals of the cyclopentadienyl rings and the orbitals of the central metal ion. A quantitative theory of the chemical bond in sandwich compounds was subsequently developed by a group of workers[2-6]. A survey of the early theories can be found in a monograph[7]. These theories are based on the consideration of the symmetry of the molecular orbitals of the ligand and the orbitals of the metal. The molecular orbitals of each cyclopentadienyl ring are formed by five atomic $2p_z$ orbitals, which can be divided into three groups differing in their symmetry relative to rotation about an axis perpendicular to the plane of the five-membered ring and passing through its centre. In order of increasing energy, the above orbitals are designated by a_1, e_1, and e_2, the symbols being related to the symmetry properties. The single a_1 orbital has no nodal planes perpendicular to the plane of the ring, while e_1 and e_2 are degenerate orbitals which do have nodal planes—one in e_1 and two in e_2. Linear combinations of these localised molecular orbitals give rise to the set of molecular orbitals a_{1g}, a_{2u}, e_{1g}, e_{1u}, e_{2g}, and e_2u embracing both cyclopentadienyl rings. The orbitals belong to the symmetry point group D_{5d} to which ferrocene and other metallocenes having the structure of a pentagonal antiprism belong. As before, the symbols e and a refer to the degenerate and non-degenerate states. The subscripts 1 and 2 define the number of nodal planes in the e-type orbitals. The additional subscripts g and u indicate the symmetry properties of the new orbitals as regards inversion relative to the centre of the molecule, i.e. relative to the metal atom. Such transformation either leaves the sign of the orbital unchanged (g) or alters it (u).

The metal orbitals 3d, 4s, and 4p can also be classified as belonging to the symmetry point group D_{5d} with the aid of the representations $a_{1g}(3d_{z^2})$, $a_{1g}(4s)$, $a_{2u}(4p_z)$, $e_{1g}(3d_{xz}, 3d_{yz})$, $e_{2g}(3d_{xy}, 3d_{x^2y^2})$, and $e_{1u}(4p_x, 4p_y)$.

The classification of the ring and metal orbitals in terms of their symmetries makes it possible to determine the combinations which contribute to the bonding states. Only those ring and metal orbitals which belong to the same representation can contribute to the overall overlap and only these combinations will lead to the formation of a metal–ring bond.

All the remaining combinations are orthogonal. The following orbitals of the cyclopentadienyl (Cp) rings and metal (M) orbitals have the appropriate symmetries: $a_{1g}(\mathrm{Cp}) - 4s(\mathrm{M})$; $a_{1g}(\mathrm{Cp}) - 3d_{z^2}(\mathrm{M})$; $e_{1g}(\mathrm{Cp}) - 3d_{xy,\,yz}(\mathrm{M})$; $e_{2g}(\mathrm{Cp}) - 3d_{xy,\,x^2-y^2}(\mathrm{M})$: $e_{1u}(\mathrm{Cp} - 4p_x(\mathrm{M})$; $a_{2u}(\mathrm{Cp}) - 4p_z(\mathrm{M})$. The electronic configuration of the complex can be represented as follows: $[a_{1g}(\mathrm{Cp})]^2$, $[a_{2u}(\mathrm{Cp})]^2$, $[e_{1u}(\mathrm{Cp})]^4$, $[3d_{z^2}(\mathrm{M})]^2$, $[3d_{xy}(\mathrm{M})]^2$, $[3d_{x^2-y^2}(\mathrm{M})]^2$, $[e_{1g}(\mathrm{Cp}) - 3d_{xz}(\mathrm{M})]^2$, and $[e_{1g}(\mathrm{Cp}) - 3d_{yz}(\mathrm{M})]^2$. (We may note that the energy levels of the electrons in the cyclopentadienyl rings are below the energy levels of the metal electrons.) Since several such combinations are allowed by the symmetry, the determination of the relative contribution of each combination to the metal–ring bond energy requires the calculation of the

overlap integrals and the determination of the relative energies of the combining states.

The principal results of the theoretical calculation are the disposition of the energy levels and the distribution of electron density. In the paramagnetic complexes the outer orbital is half-filled. The magnetic properties of the complex depend on whether the unpaired electron occupies the d_{xy}, $d_{x^2-y^2}$ orbitals (the projection of the orbital moment $M_z = \pm 2$), the d_{xz}, d_{yz} orbitals ($M_z = \pm 1$), or the d_{z^2} orbital ($M_z = 0$). The degeneracy of the d_{xy}, $d_{x^2-y^2}$ and d_{xz}, d_{yz} orbitals should be manifested in the corresponding deviations of the g-factor of the complex from its spin-only value. When the nucleus of the transition metal atom or the nuclei of the ligand atoms have magnetic moments, the hyperfine splittings in the EPR spectra or the magnetic shifts in the NMR spectra can serve as a measure of the unpaired electron density at the corresponding atoms. Fig. 1 illustrates schematically the formation of molecular orbitals by means of a linear combination of the 3d orbitals of the metal and the $2p_z$ orbitals of the carbon atoms of the cyclopentadienyl rings. Fig. 2 presents a diagram of the upper levels of the cyclopentadienyl complexes of Mn, Fe^+, Co, and Ni^+.

II. MAGNETIC PROPERTIES AND THE CHARACTERISATION OF THE EPR AND NMR SPECTRA OF PARAMAGNETIC SANDWICH COMPOUNDS

The study of magnetic susceptibility makes it possible to measure the effective magnetic moment of the molecule, to obtain information about the number of unpaired electrons, and to draw inferences about the properties of the ground state and about the fraction of the orbital component in the measured magnetic susceptibility from the deviation of the effective magnetic moment from the spin-only value. Table 1 presents the magnetic moments of metallocenes and Table 2 those of the diarene complexes.

A change in the oxidation state of the metal atom leads to the transformation of the diamagnetic complexes into paramagnetic complexes and hence permits the application of the EPR method to the study of the electronic structures of sandwich compounds.

A general discussion of the magnetic and magnetic resonance properties of sandwich compounds can be found in the paper of Robertson and McConnell[8]. The characteristics of these compounds are wholly determined by the nature of the central metal atom. In the case of orbital degeneracy (the unpaired electron occupies an e-type orbital), the effective magnetic moment and the g-factor are determined by spin–orbital coupling, by a low-symmetry distortion of the system, and by static and dynamic Jahn–Teller effects. Naturally the contribution of each of the above interactions to the splitting of the degenerate levels is different and depends on the nature of the metal.

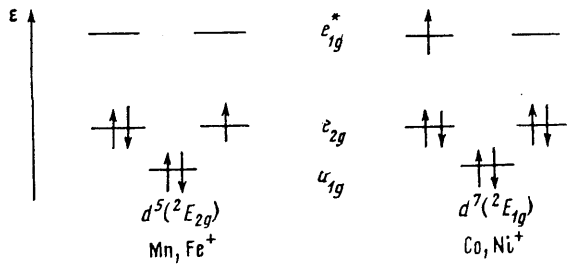


Figure 2. The energy levels of the d electrons in metallocenes.

Table 1. Experimental (μ_{eff}) and spin-only (μ) magnetic moments of metallocenes[8].

Metallocene	μ_{eff}, μ_B	S	μ, μ_B
Vanadocene	3.84	3/2	3.87
Chromocene	3.20	1	2.83
Ferrocenium cation	2.61	1/2	1.73
Manganocene	5.71	5/2	5.91
Cobaltocene	1.76	1/2	1.73
Nickelocene	2.86	1	2.83

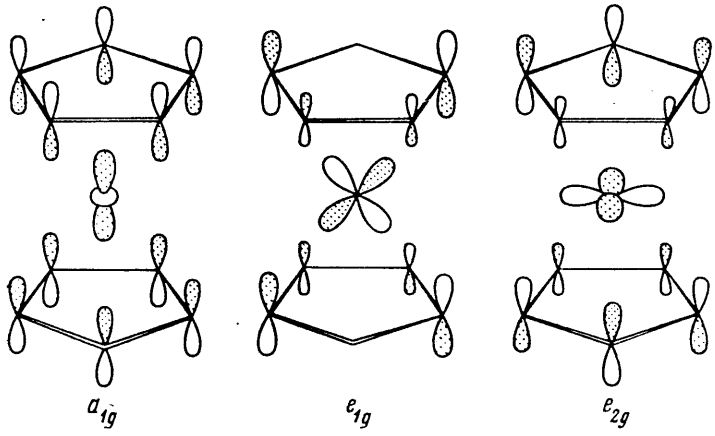


Figure 1. Schematic representation in terms of symmetry characteristics of the valence 3d orbitals of the metal and the molecular orbitals of cyclopentadienyl involved in a linear combination.

For complexes in which the unpaired electrons are distributed among the degenerate orbitals, larger deviations of the g-factor from the value for the free electron are observed. A small splitting of the degenerate levels leads to the appearance of short spin–lattice relaxation times; low temperatures (4–20 K) are required for the observation of EPR in such complexes.

Table 2. Magnetic moments of the diarene complexes of metals[24].

Complex	μ^{*}_{eff}, μ_B	S
Dibenzenevanadium	1.68	1/2
Dimesitylvanadium cation	2.80	1
Dibenzenechromium cation	1.77	1/2
Bishexamethylbenzeneiron cation	1.89	1/2
Bishexamethylbenzeneiron	3.08	1
Bishexamethylbenzenecobalt dication	1.73	1/2
Bishexamethylbenzenecobalt cation	2.95	1
Bishexamethylbenzenecobalt	1.86	1/2
Bishexamethylbenzenenickel dication	3.00	1

*The spin-only moments μ are 1.73 and 2.83 for $S = 1/2$ and $S = 1$ respectively.

The presence of more than one unpaired electron in the molecule leads to the splitting of the levels in a zero external magnetic field as a consequence of the interaction between the unpaired electrons. Such splitting sometimes constitutes an additional difficulty in the observation of EPR. Since zero field splitting can greatly exceed the attainable energy microwave quanta, EPR cannot be observed. In such cases, the observation of EPR is impossible and the application of NMR, which is not subject to the above limitations is particularly valuable. In the NMR spectra of complexes with short electron spin–lattice relaxation times, lines which are relatively narrow for paramagnetic specimens are observed. In the case of systems with a large zero field splitting, NMR is the only feasible microwave spectroscopic research technique.

The hyperfine structure (HFS) of the EPR spectra, the zero field splitting of the signal, and the paramagnetic shift of the NMR lines are important sources of information about the distribution of the unpaired electron density. In the EPR spectra of metallocenes and diarene complexes, a hyperfine structure, which depends on the nature of the metal and is due to the interaction of the unpaired electron with the magnetic moment of the metal nuclei and the ligand protons, is observed. Analysis of the HFS in the solid phase (in single crystals or in vitrified solutions) makes it possible to determine values of the hyperfine interaction (HFI) tensor as well as the isotropic HFI constant which enters into the so-called contact paramagnetic shift of the NMR line.

Under the conditions of rapid electron spin–lattice relaxation, the contact shift $\Delta\nu$(Hz) of the NMR line is described by the equation

$$\Delta\nu/\nu_0 = -Ag_{av}\beta_e S(S+1)/g_N\beta_N(3kT),$$

where A is the constant of the isotropic hyperfine interaction of the unpaired electron with the corresponding nucleus, $g_{av} = 1/3(g_\parallel + 2g_\perp)$, β_e and β_N are the electronic and nuclear magnetons, g_N is the nuclear spectroscopic splitting factor, S the spin of the paramagnetic complex, k the Boltzmann constant, and T the temperature on the Kelvin scale. The above formula shows that the temperature variation of the contact shift is consistent with the Curie law[9]. Hence it follows that only when this law holds is it possible to calculate A from the slope of the plot of $\Delta\nu$ against $1/T$.

The expression for the constant A is

$$A = \frac{8\pi}{6S} g_e\beta_e g_N\beta_N |\psi(0)|^2 ,$$

where $|\psi(0)|$ is the molecular wave function of the unpaired electron at the nucleus. Thus the contact shift carries potentially the same information about the distribution of the unpaired electron density in the paramagnetic complex as the isotropic HFI constant obtained from the EPR spectra. The study of the contact shifts of the NMR lines is of particular value in view of the fact that, apart from the determination of the constant A, it also yields its sign. This permits in its turn the determination of the sign of the spin density at the corresponding atom. The determination of the magnitudes and signs of the spin density permits conclusions concerning the mechanism of the delocalisation of the unpaired electron in the complexes.

When the anisotropy of the g-factor is considerable, the pseudocontact shift[9], arising as a result of the dipole–dipole interaction of the magnetic moment of the unpaired electron with the magnetic moment of the corresponding nucleus at a distance r, makes a contribution, apart from the contact shift, to the experimental paramagnetic shift. The form of the expressions describing the contribution of the pseudocontact shift depends on the ratio of the correlation times of the rotational mobility τ_2 (τ_2 is the time of the rotation of the complex by one radian), the characteristic time determined by the anisotropy of the g-factor, and the electron spin–lattice relaxation time T_1.[10] Two cases are distinguished:

(a) $1/\tau_2 \ll |g_\parallel - g_\perp|\beta H/\hbar$, $T_1 \ll \tau_2$, $\Delta\nu/\nu_0 = \Gamma(g_\parallel^2 - g_\perp^2)/3$;

(b) $1/\tau_2 \gg |g_\parallel - g_\perp|\beta H/\hbar$, $T_1 \ll \tau_2$, $\Delta\nu/\nu_0 = \Gamma(3g_\parallel + 4g_\perp)(g_\parallel - g_\perp)/15$,

where Γ is the so-called geometrical factor taking into account the relative positions of the unpaired electron and the nucleus:

$$\Gamma = -\frac{\beta^2 S(S+1)}{3kT}\left\langle\frac{3\cos^2\varphi - 1}{r^3}\right\rangle .$$

Proton magnetic resonance spectroscopy has been supplemented in recent years by the ^{13}C magnetic resonance spectroscopy. The application of ^{13}C NMR greatly extended the scope of the study of paramagnetic complexes and made it possible to construct a map of the spin density distribution incorporating all the atoms of the complex. Analysis of the spin density distribution makes it possible to estimate the relative involvement of the metal and ligand atoms in the molecular orbital of the unpaired electron, which is important for understanding the nature of the bond in sandwich metal complexes.

1. EPR and NMR Spectra of Sandwich Compounds of Iron

The first EPR spectra of the ferrocenium cation were not obtained until 1969[11], much later than the EPR spectra of the sandwich compounds of other metals. The difficulties in the study of the EPR spectra of ferrocenium and its derivatives are associated with the short spin–lattice relaxation time T_1, which hinders measurements at temperatures above 77 K. The EPR spectra of the ferrocenium cation and its derivatives have been recorded at 20 K in dimethylformamide. Fig. 3 presents the EPR spectra of $Fe(C_5H_5)_2I_3$, $CH_3C_5H_4Fe.C_5H_5I_3$, and $(CH_3C_5H_4)_2FeI_3$. Table 3 presents the values of $g_\parallel$, $g_\perp$, the line widths $\Delta H_\parallel$ and $\Delta H_\perp$, as well as certain

parameters characterising the electronic state of the ferrocenium cation[12]. The line width $\Delta H_\perp$ was measured between the peaks and $\Delta H_\parallel$ was measured at the level of half the height of the signal corresponding to $g_\parallel$. It follows from the data in Table 3 that the introduction of substituents lowers $\Delta H_\perp$ by a factor greater than ten.

Table 3. EPR parameters* of the ferrocenium cation and its derivatives[15].

Substituent	$g_\parallel$	$g_\perp$	$\Delta H_\parallel$, G	$\Delta H_\perp$, G	K	X	δ, cm^{-1}
H	4.35	1.26	140	2500	0.76	1.23	270
CH_3	4.17	1.47	160	1500	0.80	0.92	360
C_6H_5	3.98	1.58	180	850	0.80	0.78	420
1,1'-di-CH_3	3.83	1.67	160	450	0.83	0.66	500
1,1-di-C_4H_9	3.88	1.68	230	600	0.86	0.65	500
C_6H_5CO	3.69	1.73	140	300	0.84	0.58	570
1,1'-di-C_6H_5	3.63	1.74	160	300	0.82	0.57	580
CH_3CO	3.62	1.76	130	220	0.85	0.54	610

*Notation: K is the fraction of the unpaired electron density on the iron atom; $X = \xi/\delta$, where ξ is the spin–orbit coupling constant: δ = energy of the splitting of the e_{2g} level in a low-symmetry field.

Ligand field theory predicts the sequence of the levels of the five degenerate orbitals of the transition metal ion[8], illustrated schematically in Fig. 2. This sequence arises as a result of the influence of the field of the cyclopentadienyl rings on the metal ion orbitals. As a consequence of symmetry properties, the orbital $e_{1g}(3d_{\pm1})$ and $e_{2g}(3d_{\pm2})$ remain degenerate. Since ferrocene is diamagnetic, it has the low-spin configuration $^1A_{1g}(e_{2g})^4(a_{1g})^2$. The distance between the e_{1g} and a_{1g}, e_{2g} orbitals is fairly large and exceeds the exchange interaction energy stabilising the high-spin configuration of the d^6 level.

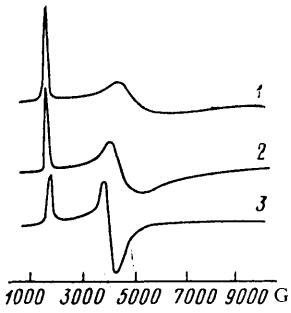


Figure 3. EPR spectra of ferrocenium cations in dimethylformamide at 20 K: 1) $Fe(C_5H_5)_2I_3$; 2) $Fe(C_5H_5)(C_5H_4CH_3)I_3$; 3) $Fe(C_5H_4CH_3)_2I_3$.[15]

Measurement of the magnetic susceptibility of the $FeCp_2^+$ cation showed that it has the low-spin d^5 configuration and that its magnetic moment deviates appreciably from the spin-only value[8]. The orbitally degenerate state $^2E_{2g}(a_{1g})^2(e_{2d})^3$ has been proposed as the ground state of $Fe_2Cp_2^+$.[13,14]

A system of five d electrons has been examined theoretically[15] by replacing it by a single electron "hole" having the electronic configuration $^2E_{2g}(e_{2g})$. In an axial ligand field H_0, this configuration is quadruply degenerate—doubly degenerate for the spin functions α and β and doubly degenerate for the orbital functions e_{+2} and e_{-2}. In view of the axial symmetry of the system, the eigenfunctions of the projection operator of the orbital moment L_z, where the main molecular axis perpendicular to the plane of the ligand rings was selected as the z axis, were chosen as a basis set of wave functions. The spin–orbit interaction $\hat{H}_{SO}$ splits the quadruply degenerate level into two doubly degenerate levels: $\{e_{+2}\alpha, e_{-2}\beta\}$ with $|M_j| = 5/2$ and $\{e_2\alpha, e_{+2}\beta\}$ with $|M_j| = 3/2$. The energies of these states differ by 2ξ, where ξ is the spin–orbit coupling parameter. For the electron "hole", ξ is negative and the doublet with $|M_j| = 5/2$ refers to the ground state of the unpaired electron. This doublet is located several hundreds of cm^{-1} below the doublet with $|M_j| = 3/2$.

$$g_\parallel = 2\langle e_{+2}\alpha|l_z + 2S_z|e_{+2}\alpha\rangle = 2 + 4K\,,$$
$$g_\perp = 2\langle e_{+2}\alpha|l_x + 2S_x|e_{-2}\beta\rangle = 0\,,$$
$$K = \tfrac{1}{2}\langle e_{+2}|l_z|e_{+2}\rangle\,.$$

The result $g_\perp = 0$ implies that, to a first approximation, the levels to which the ground state doublet corresponds are not split by a magnetic field parallel to the x and y axes. On the other hand, the probability of the EPR transitions in the case where the magnetic field is parallel to the z axis is $\langle e_{+2}\alpha|S_x|e_{-2}\beta\rangle = 0$. Hence it follows that the EPR spectrum of the ferrocenium cation should not be observed. On the basis of the results obtained, the author[15] concludes that the symmetry of the cation $FeCp^+$ is lower than the axial symmetry and this explains the presence of the EPR signal.

The decrease of the symmetry of the cation $FeCp_2^+$ may be induced by the solvent molecules, the anion, or the distortion due to the Jahn–Teller effect; in substituted $FeCp_2^+$ the symmetry can also be reduced by the influence of the substituent.

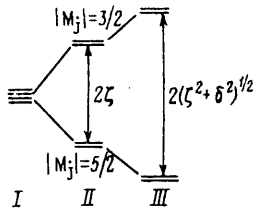


Figure 4. Diagram of the $^2E_{2g}$ levels of the ground state of $Fe(C_5H_5)_2^+$: I) in the axial field of the ligand; II) in the axial field of the ligands with superposition of the spin–orbit coupling (2ξ); III) in the axial field with superposition of spin–orbit coupling and a low-symmetry field (δ).

The overall Hamiltonian $\hat{H}$, describing the behaviour of the unpaired electron, can be represented by the sum of the effective one-electron Hamiltonian $\hat{H}_0$, corresponding to the axial symmetry of the complex, and the terms $\hat{H}_{SO}$ and $\hat{H}_1$ associated respectively with the spin–orbit coupling and the interaction with a low-symmetry field. The latter interaction removes the degeneracy and splits the e_{2g} level into two components, $e_{x^2-y^2}$ and e_{xy}, separated by a distance $\sim 2\delta$. It may be expected that $\hat{H}_1$ and $\hat{H}_{SO}$ are of the same order of

magnitude and that the determination of the splitting requires the solution of the secular equation. The solution of the secular determinant yields two doubly degenerate levels whose location is illustrated in Fig.4.

$$\Psi_1 = (\cos\varphi \cdot e_{x^2-y^2} + i \sin\varphi \cdot e_{xy})\alpha \ ,$$
$$\Psi_2 = (\cos\varphi \cdot e_{x^2-y^2} - i \sin\varphi \cdot e_{xy})\beta \ ,$$

where $\tan\phi = (1 + 1/X^2)^{1/2} - 1/X$ and $X = -\xi/\delta$. The energy of the lower doublet level corresponding to these functions is $-(\xi^2 + \delta^2)^{1/2}$ and the energy of the upper doublet is $+(\xi^2 + \delta^2)^{1/2}$. New values of the g-factors were calculated using these wave functions[15]:

$$g_z = 2\langle\Psi_1|l_z + 2S_z|\Psi_1\rangle = 2 + \frac{4KX}{(1+X^2)^{1/2}} \ ,$$
$$g_x = g_y = 2\langle\Psi_1|l_x + 2S_x|\Psi_2\rangle = \frac{2}{(1+X^2)^{1/2}} \ .$$

The parameters K and X can be determined from the two equations for g_z and $g_x = g_y$.

The orbital $|e_{+2}\rangle$ is a linear combination of the 3d orbital of the iron atom and the ligand π orbital L_π, which is a linear combination of the $2p_z$ orbitals of the carbon atoms in the cyclopentadienyl rings:

$$|e_{+2}\rangle = C_1|3d_{+2}\rangle + C_2|L_\pi\rangle \ .$$

Substitution in the equation for K yields the following expression:

$$K = \frac{1}{2}\langle e_{+2}|l_z|e_{+2}\rangle =$$
$$= C_1^2 + C_1C_2\langle 3d_{+2}|l_z|L_\pi\rangle + \frac{1}{2}C_2^2\langle L_\pi|l_z|L_\pi\rangle \ .$$

As the initial approximation it was assumed that the orbital moment associated with the ligand electrons is to a large extent extinguished[15] and for this reason the last two integrals were assumed to be zero. Hence it follows that $K = C_1^2$. It is seen from the data in Table 3 that the average $K = 0.82$ and $C_1 = 0.91$, which shows that the 3d orbital of the iron atom makes the main contribution to the e_{2g} orbital of the complex and that the unpaired electron is localised mainly at the iron atom. Calculations of the molecular orbitals carried out for ferrocene predict the same results. Values in the range 0.85–0.91 were found for C_1.[2-4]

The splittings of the energy levels in a low-symmetry field $\hat{H}_1$ can be determined from the parameter X. Since $\delta = -\xi/X$ and $\xi = C_1^2\xi_0$, where $\xi_0 = 400$ cm^{-1}, the spin–orbit coupling constant for the Fe^{3+} cation is $C_1 = 0.82$. The results obtained show that the axial symmetry is infringed even in the unsubstituted ferrocenium cation. The high value $\delta = 270$ cm^{-1} leads to the conclusion that the infringement of the symmetry is associated with external factors[15].

The similarity of the energies of the states with $|M_j| = 3/2$ and $|M_j| = 5/2$ explains the short spin–lattice relaxation time of the ground state. The energy difference $\Delta E = 2(\xi^2 + \delta^2)^{1/2}$ of the states with $|M_j| = 5/2$ and 3/2 is 860 cm^{-1} in $FeCp_2^+$, 1200 cm^{-1} in $(CH_3C_5H_4)_2Fe^+$, and 1390 cm^{-1} in $(CH_3COC_5H_4)_2Fe^+$. The order of magnitude of these quantities explains why the EPR signal of $FeCp_2^+$ is too broad to be observed at 77 K, while the EPR spectra of complexes with a higher ΔE can be observed at this temperature.

The magnetic moment of the cation $FeCp_2^+$ has been determined[15] by measuring the magnetic susceptibility ($\mu = 2.61$ μ_B in crystalline powders of ferrocenium salts and by the NMR method from the paramagnetic shift of the solvent protons ($\mu = 2.30$ μ_B). The magnetic moment obtained by NMR is in good agreement with the value calculated from EPR data:

$$\mu = \left\{\frac{1}{3}(g_\parallel^2 + 2g_\perp^2)\,S(S+1)\right\}^{1/2}\mu_B = 2.35\mu_B \ .$$

The apparent conflict between the results of the theoretical analysis of the distortion of the axial symmetry of $FeCp_2^+$ and the equality of g_x and g_y obtained from the EPR spectrum is due to the fact that the difference $g_x - g_y$ is proportional to $\xi/\Delta E_i$, where $\Delta E_i = E(e_1g) - E(e_2g) \cong 30000$ cm^{-1} is unduly small compared with the line width in the EPR spectrum.

Simultaneously with Prins' communication[15], the study of Horsfield and Wassermann[16], dealing with the same problem, was published. They investigated the EPR spectra of $FeCp_2^+$ trichloroacetate, picrate, and chloride at 77 K. The g-factors obtained differ appreciably ($g_\parallel \cong 3.20$; $g_\perp \cong 1.80$) from Prins' data[15]. In the subsequent discussion, attention was drawn to the instability of the ferrocenium cation[17,18] and the possible formation of paramagnetic impurities. The additional studies which followed the discussion[18] established that the signals recorded by Horsfield and Wassermann are observed in freshly prepared specimens at 77 K, but, on reducing the temperature to 20 K, the more intense signals with the values of $g_\perp$ and $g_\parallel$ obtained by Prins are recorded[15].

Theoretical calculations and experimental EPR spectra of the ferrocenium cation have shown that the main contribution to the orbital of the unpaired electron of the cation comes from the 3d orbital of the metal atom. The shift of the unpaired electron to the ligands might be indicated by the hyperfine structure of the spectrum due to the interaction with the protons of the cyclopentadienyl rings. Since A_H is much smaller than the width of the EPR line, this information cannot be obtained from the EPR spectrum. It was obtained with the aid of NMR.

Fritz et al.[19] were the first to investigate the NMR of the ferrocenium cation and its alkyl derivatives. They measured the paramagnetic shifts of the signals due to the protons in the cyclopentadienyl ring and the protons of the α-CH_2, β-CH_2, and γ-CH_3 groups in the substituted ferrocenium cation. The paramagnetic shifts $\Delta\nu$ (p.p.m.) measured at a frequency of 100 MHz proved to be small:

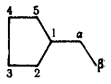
Cp ring	α-CH_2	β-CH_2	γ-CH_3
$-(30-16)$	15 — 18	7	0

The results obtained indicate quantitatively a low unpaired electron density in the ligand orbitals. However, the constants for the isotropic HFI between the unpaired electron and the protons cannot be calculated directly from the paramagnetic shifts because of the contributions to $\Delta\nu$ by the pseudocontact shift. Attempts have been made in a number of studies to separate the contact and pseudocontact contributions[15,19,20]. The inaccuracy of the first attempts was due to the insufficiency of the EPR data and data concerning the structure of the ferrocenium cation[15,19].

It has been found[20] that the dipole contribution to the observed paramagnetic shifts of the signal due to the methyl protons of the cation $Fe(C_5H_4CH_3)_2^+$ is ~55% and the contribution to the paramagnetic shift of the protons of the cyclopentadienyl rings is 25%. The calculated isotropic HFI constants are $A_H = 0.168$ G for $Fe(C_5H_5)_2^+$ and $A_H = 0.161$ G and $A_{CH_3} = 0.095$ G for $Fe(C_5H_4CH_3)_2^+$.

A more thorough analysis of the temperature variation of the paramagnetic shift[21] showed that this variation is different for the protons of the cyclopentadienyl rings of $FeCp_2^+$ and $(RC_5H_5)_2Fe^+$. Whereas in the case of $FeCp_2^+$ the Curie law hold rigorously, deviations are observed for the protons of the $(RC_5H_4)_2Fe^+$ rings. Köhler[21] concluded that the protons in substituted cyclopentadienyl rings are non-equivalent, which leads to the observed deviations in the temperature variation. This hypothesis has been confirmed. The application of ^{13}C NMR showed that the carbon atoms in the cyclopentadienyl rings of $(RC_5H_4)_2Fe^+$ are non-equivalent[22].

Table 4 presents the paramagnetic shifts of the ^{13}C NMR of the ferrocenium cation and some of its alkyl derivatives.



In conformity with the signs of the paramagnetic shifts of the NMR lines of the ^{13}C and ^{1}H nuclei, the signs of the spin density on the corresponding atoms can be obtained. The spin densities on the carbon and hydrogen atoms of the cyclopentadienyl rings have the positive sign. The positive sign of the shift of the proton signal of the CH_3 group in $Fe(C_5H_4CH_3)_2^+$ is due to the fact that the positive pseudocontact shift is greater in absolute magnitude than the negative contact shift[20]. Thus, although the spin densities on the carbon nuclei are in fact positive, the ^{1}H NMR line of the CH_3 group is displaced upfield.

Table 4. Shifts of the ^{13}C NMR lines (p.p.m.) in the spectrum of ferrocenium hexaphosphate in acetone at 28 °C.[22]

Ferrocenium cation	C(1)	C(2, 5), C(3, 4)	C^{α}	C^{β}
$(C_5H_5)_2Fe^+$	—	−314.5	—	—
$(CH_3C_5H_4)_2Fe^+$	−415	−263.0	+10	—
$(C_2H_5C_5H_4)_2Fe^+$	−402.5	−259.8	+0.5	+9.2
$(C_4H_9C_5H_4)_2Fe^+$	−414.0	−233.6 −250.6	−16.3	+3.9

The bis(hexamethylbenzene)iron cation is an example of a 19-electron system (d^7). Three signals, corresponding to three values of the g-factor, are observed in the EPR spectrum: $g_x = 1.865$, $g_y = 1.996$, and $g_z = 2.086$.[23] It is of interest that there is no axial symmetry in such a highly symmetrical molecule. The absorption signal is observed in the range from 25 to 80 K, disappearing at 90 K owing to the considerable broadening of the line. It has been suggested[23] that the unpaired electron occupies the non-bonding ligand orbital e_{2u}. Subsequent study of the NMR spectra of this compound showed that the unpaired electron density on the ligands is low[24]. This result is inconsistent with the hypothesis that the unpaired electron is located in the e_{2u} orbital. It is most likely that the electron occupies the e_{1g}^* orbital of the iron atom.

The electrically neutral arenecyclopentadienyliron complexes also belong to d^7 systems. The reduction of the salts $[AreneFeC_5H_5]^+BF_4^-$ in 1,2-dimethyoxyethane at −70 °C on a sodium mirror leads to the transformation of the d^6 system, isoelectronic with ferrocene, into the d^7 system $a_{1g}^2e_{2g}^4(e_{1g}^*)^1$.[25]

The doubly degenerate e_{1g}^* level is split as a consequence of the low-symmetry interaction with the arene ligand. On the assumption that the unpaired electron occupies mainly one of the two orbitals d_{xz} or d_{yz}, expressions were obtained for $g_{\parallel}$ and $g_{\perp}$:

$$g_z = g_{\parallel} = 2\left(1 - \frac{\lambda_0}{\Delta E}\right);\ g_x = g_y = g_{\perp} = 2,$$

where

$$\Delta E(e_{1g}^*) = E_{d_{xz}} - E_{d_{yz}}, \quad \text{and} \quad \lambda_0(Fe^+) = -350\ cm^{-1}.$$

Table 5 presents the values of $g_{\parallel}$ for electrically neutral arenecyclopentadienyliron complexes (the values of $g_{\perp}$ for all the compounds are close to 2). The table shows that $g_{\parallel}$ decreases in the sequence of ligands benzene, naphthalene, phenanthrene. The values of $\Delta E(e_{1g}^*)$ for benzene, naphthalene, and phenanthrene are respectively 2700, 7700, and 10000 cm^{-1}. The increase of $\Delta E(e_{1g}^*)$ can be attributed to the increase of the electron-donating capacity of the ligands in this sequence, leading to the enhancement of the interaction of the ligands with the iron atom on which there is a positive charge.

Table 5. The values of $g_{\parallel}$ for electrically neutral arenecyclopentadienyliron complexes[25].

Arene	$g_{\parallel}$	Arene	$g_{\parallel}$	Arene	$g_{\parallel}$
Benzene	2.26	Tetralin	2.21	Fluorene*	2.10
Toluene	2.25	Dihydroanthracene	2.22	Naphthalene	2.09
Diphenylmethane	2.24	Mesitylene	2.24	Phenanthrene	2.07
p-Xylene	2.25	Durene	2.21		

*Breakdown of axial symmetry: $g_x = 2.00$; $g_y = 1.99$.

The study of the EPR spectra of the dications $[AreneFeC_5H_5]^{2+}$,[26] obtained by oxidising the initial salts $SbCl_5$ in CH_2Cl_2 at −70 °C, can yield data about the d^5 system which is isoelectronic with the ferrocenium cation[15]. Table 6 presents the values of $g_{\parallel}$, $g_{\perp}$, and $\Delta E(e_{2g}) = E_{d_{x^2-y^2}} - E_{d_{xy}}$:

$$g_z = g_{\parallel} = 2\left(1 - \frac{2\lambda_0}{\Delta E(e_{2g})}\right);\ g_x = g_y = 2;\ \lambda_0 = -400\ cm^{-1}.$$

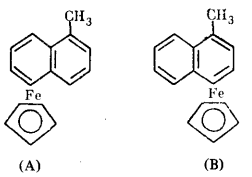
Evidently, the splittings $\Delta E(e_{1g}^*)$ are much greater than $\Delta E(e_{2g})$. This result reflects the greater "π character of the d_{xz} and d_{yz} orbitals and their more effective overlap with the molecular π orbitals of the ligands compared with the $d_{x^2-y^2}$ and d_{xy} orbitals. Comparison of the data in Table 6 with the parameters of the EPR spectra of ferrocenium cations (Table 3) shows that the low-symmetry splitting in the dications $[AreneFeC_5H_5]^{2+}$ is much greater than in ferrocenium cations.

Table 6. The values of $g_{\parallel}$, $g_{\perp}$, and $\Delta E(e_{2g})$ for the EPR spectra of arenecyclopentadienyliron dications[26].

Arene	$g_{\parallel}$	$g_{\perp}$	$\Delta E(e_{2g})$, cm^{-1}
$CH_3OC_6H_5$	3.14	1.940	1400
$C_6H_5OC_6H_5$	3.14	1.920	1400
p-$FC_6H_4C_6H_5$	3.16	1.898	1380
$C_6H_5C_6H_5$	3.04	1.930	1540
$C_{10}H_8$	2.80	1.976	2000
β-$FC_{10}H_7$	2.83	1.976	1930
α-$CH_3C_{10}H_7$ (A)	2.81	1.977	1970
α-$CH_3C_{10}H_7$ (B)	2.71	1.988	2260
$C_{14}H_{10}$	2.86	1.964	1860

It is of interest to compare the data for $[C_{10}H_8FeC_5H_5]^{2+}$, $[\alpha\text{-}CH_3C_{10}H_7FeC_5H_5]^{2+}$, and $[\beta\text{-}FC_{10}H_7FeC_5H_5]^{2+}$. Table 6 shows that the signal corresponding to $g_{\parallel}$ in the $[\alpha\text{-}CH_3C_{10}H_7.FeC_5H_5]^{2+}$ spectrum is split into two components. A smaller splitting is observed also in the signal corresponding to $g_{\perp}$.

We attributed this feature of the $[\alpha\text{-}CH_3C_{10}H_7FeC_5H_5]^{2+}$ spectrum to the existence of two different isomers[26]:



(A) (B)

This hypothesis is confirmed by the NMR data for the cations $[\beta\text{-}CH_3C_{10}H_7FeC_5H_5]^+$ and $[\alpha\text{-}FC_{10}H_7FeC_5H_5]^+$.[27] The ratio of isomers (A) and (B) for the former cation is 55:45 while for the latter cation only isomer (A) is observed.

2. The EPR and NMR Spectra of Sandwich Compounds of Vanadium

The EPR spectrum of VCp_2 has been investigated[28] for a single crystal of diamagnetic $FeCp_2$ and the splitting parameter in a zero magnetic field $D = 0.83$ cm^{-1} was determined for the quartet ground spin state. On the other hand, the EPR spectrum obtained previously[29] in benzene solution at room temperature and consisting of eight well resolved lines ($A_V = 25.6 \times 10^{-4}$ cm^{-1}) with $g = 2.00$ was also attributed to vanadocene. These data are in conflict, since a much greater width of the spectral line recorded in solution is to be expected for such a high value of D.

The EPR spectrum of VCp_2 in vitrified solution in 2-methyltetrahydrofuran has been investigated[30] at 77 K and it has been shown that the signal observed in solution at room temperature is due to an impurity. The VCp_2 signal observed at 77 K is characterised by the parameters $g_\parallel = 2.002$, $g_\perp = 1.99$, $|D| = 2.3$ cm^{-1}, $|A| = 3.7 \times 10^{-4}$ cm^{-1}, and $|B| = 21 \times 10^{-4}$ cm^{-1}.[30] The difference between the given value of $|D|$ and that obtained in another study[29] was attributed[30] to the differences between the matrices in which the EPR spectra of VCp_2 were recorded. The similarity of the measured g-factor to the value for the free electron is consistent with measurements of the magnetic susceptibility and shows that the ground state for vanadium is an orbital singlet $^4A_{1g}$ and corresponds to the configuration $a_{1g}^1 e_{2g}^2$.

On the assumption that a_{1g} is a non-bonding metal orbital, the parameters of the hyperfine interaction tensor can be expressed by the formulae

$$A = A_{iso} - \frac{4}{21} P (2\alpha^2 - 1);\ B = A_{iso} + \frac{2}{21} P (2\alpha^2 - 1),$$

where α is the contribution of the e_{2g} orbital of the metal to the molecular orbital and $P = 2\gamma_e \beta_e \beta_N \langle r^{-3} \rangle$. For $P = 110 \times 10^{-4}$ cm^{-1}, it was found that $\alpha = 0.86$.[30]

Rettig and Drago[9] investigated the NMR spectrum of VCp_2 in toluene at a frequency of 60 MHz and found that the paramagnetic shift of the ring proton signal is −18500 Hz relative to the protons of the diamagnetic dimethylferrocene, i.e. ~300 p.p.m. An estimate of the contribution of the pseudocontact shift showed that it is an insignificant proportion of the overall shift observed experimentally. The temperature variation of the shift obeys the Curie law. The isotropic HFS constant is 0.832 G.

The contact shifts in 1,1-dimethylvanadocene are −20190 G for the protons of the cyclopentadienyl rings and 7195 G for the protons of the methyl group. The constant for the hyperfine interaction with the protons of the methyl group, determined from the NMR data, is 0.323 G.[9]

Comparison of the values and signs of the contact shifts of the ring and methyl group protons has been used[9] to determine the mechanism of the displacement of the unpaired electron density from the metal atom to the ligand. The mechanism of the delocalisation of the unpaired electron in paramagnetic metallocenes proposed previously[13] presupposes the involvement of the 3d orbitals of the metal atoms and the π orbitals of the ligand as well as the spin polarisation of the CH bonds in the ring. The main contradiction between this theory and the experimental data obtained from the NMR spectra of VCp_2 is that the mechanism of the spin polarisation developed by Levy and Orgel[13] in relation to the π-electron free radicals presupposes different signs of the HFI constant for the protons of the CH bond and of the CH_3 group, while their absolute magnitudes are approximately equal. However, in the case of vanadocene the signs of the experimental HFI constants for the ring and methyl group protons are the same, while their absolute values differ greatly—the HFI constant for the ring protons exceeds in absolute magnitude the HFI constant for the methyl group protons by a factor greater than two. The markedly lower HFI constants for the protons of the alkyl substituent compared with the HFI constant for the ring protons had already been noted earlier in a study of the EPR spectra of the cations of alkyl derivatives of dibenzenechromium[31].

Rettig and Drago[9] suggested that the principal mechanism for the transfer of spin density from the central metal atom in individual metallocenes to the ligand protons involves transfer via σ and not π bonds. A characteristic feature of this mechanism is a marked decrease of spin density along the chain of σ bonds and the identical signs of the constants of the hyperfine interaction with the protons of the CH bonds and the CH_3 groups.

^{13}C NMR data for vanadocene and 1,1-dimethylvanadocene have shown that the delocalisation pattern is much more complex[32]. Table 7 presents the contact shifts of the ^{13}C and ^1H NMR signals for vanadocene and its alkyl derivatives. The positive shift of the signal from the ^{13}C atom in the ring implies that the unpaired electron spin density on the ring carbon atoms has a negative sign. The negative sign of the contact shift of the ring protons supports the spin polarisation mechanism and is an argument against the mechanism involving delocalisation via σ bonds.

Table 7. Paramagnetic shifts (p.p.m.) of the ^{13}C and ^1H NMR lines of vanadocene, chromocene, and their alkyl derivatives[32].

Compound	C(1)	C(2,5)	C(3,4)	C^α	C^β	H(2,5)	H(3,4)	H^β	H^γ
$(C_5H_5)_2V$	+588	+588	—	—	—	−315	−315	—	—
$(CH_3C_5H_4)_2V$	+482	+750	+533	−915	—	−326	−326	−116	—
$(C_2H_5C_5H_4)_2V$	+480	+743	+562	−792	−420	−340	−340	−90	−5.4
$(C_4H_9C_5H_4)_2V$	+503	+730	+533	−557	−220	—	—	—	—
$(C_5H_5)_2Cr$	+325	+325	+325	—	—	−324	−324	—	—
$(CH_3C_5H_4)_2Cr$	+68	+505	+347	−535	—	−377	−318	−37.2	—
$(C_2H_5C_5H_4)_2Cr$	+99	+488	+367	−497	−92	−357	−310	−18.0	+3.0
$(C_4H_9C_5H_4)_2Cr$	+130	+483	+368	−390	−22	−344	−312	—	—

The EPR spectra of the diarene sandwich complexes of zerovalent vanadium (with benzene, toluene, mesitylene, and naphthalene as ligands) have been investigated[33]. Hyperfine interaction with the magnetic moment of the vanadium nucleus is observed in the spectra of all these compounds, which leads to the appearance of eight HFS lines ($I_V = 7/2$) with a splitting $A_V = 63$ G. Each of the eight lines in the spectrum of the dibenzenevanadium(O) complex is additionally split into 13 lines with a binomial distribution of relative intensities as a result of the interaction with the protons of

the benzene rings: A_H = 4 G and g = 1.987.[33] The introduction of substituents into the ligands (toluene and mesitylene) does not alter the HFI constants, but merely diminishes the number of lines in the spectrum; hyperfine interaction with the protons of the CH_3 groups is not observed[34].

Analysis of the HFS spectrum of the dinaphthalenevanadium(0) complex showed that only one benzene ring of naphthalene is involved in a bond with the vanadium atom. The spectral parameters (A_V = 63 G, A_H = 4 G, g = 1.987) do not differ from those quoted above for the dibenzenevanadium(0) complex. The electronic configuration $...(e_{1u})^4 (e_{2g})^4 (a_{1g})^1$ with an unpaired electron in the $a_{1g}(3d_{z^2})$ orbital is characteristic of zerovalent vanadium complexes[35].

The results show that the delocalisation of the unpaired electron over the π bonds does not play a significant role in the diarenevanadium(0) compounds.

The paramagnetic shifts of the proton signals of the CH bonds and the CH_3 groups in the ^{1}H NMR spectra of $V(C_6H_6)_2^+$, $V(C_6H_5CH_3)^+$, and $V[C_6H_3(CH_3)_3]_2^+$ [24] (ν_0 = 60 MHz) have been measured:

Compound	$V(C_6H_6)_2^+$	$V(C_6H_5CH_3)_2^+$	$V(C_6H_3(CH_3)_3)_2^+$
A_H, G	1.13	1.34	1.23
δ_H, G	−13 990	−16 740	−16 410
A_{CH}, G	—	0.824	0.306
δ_{CH_3}, Hz	—	−8 400	−3 860

The electronic configuration $(e_{2g})^3 (a_{1g})^1$, corresponding to the degenerate $^3E_{2g}$ ground state, has been proposed on the basis of molecular orbital calculations[36].

3. EPR and NMR Spectra of Sandwich Compounds of Chromium

Nüssbaum and Voitländer[37,38] were unable to observe the EPR signals of the complex $CrCp_2$ either in the 3-cm or 8-mm wavelength range at temperatures from room temperature to 4 K; the reasons for this failure were recognised to be the large zero field splitting and the short relaxation time. The magnetic moment of chromocene greatly exceeds the value of the spin-only magnetic moment, which indicates a degenerate electronic state of the complex. According to theoretical calculations, the ground state of chromocene is $(e_{2g})^3 (a_{1g})^1$ [39] and the a_{1g} level is higher by 0.4 eV than the e_{2g} level.

The paramagnetic shift of the proton signals of chromocene in the NMR spectrum relative to the signals of the dimethylferrocene protons is −18850 Hz (ν_0 = 60 MHz), which corresponds to an HFI constant of 1.23 G.[9] In the spectrum of dimethylchromocene the lines due to the protons of the cyclopentadienyl ring are split into two components, which indicates some redistribution of the unpaired electron density in the cyclopentadienyl rings under the influence of the methyl groups. The shifts of the proton signals of the cyclopentadienyl rings are −18630 and −21896 Hz, while that of the methyl group protons is −2160 Hz. The chemical shifts correspond to the HFI constants A_H = 1.22 and 1.43 G and A_{CH_3} = 0.41 G.

Table 7 lists the contact shifts in the ^{13}C and ^{1}H NMR spectra of chromocene and its alkyl derivatives[32]. As in the case of vanadocene, the contact shift of the lines due to the carbon nuclei of chromocene has a positive sign, which indicates a negative unpaired electron spin density in the cyclopentadienyl ring. In conformity with the CH bond spin polarisation model, the spin density on the hydrogen atoms has a positive sign.

Numerous studies have been devoted to the EPR and NMR spectra of the dibenzenechromium cation and its derivatives. The EPR of dibenzenechromium was observed in 1954.[40] Subsequent investigation[31] showed that the EPR spectrum of the dibenzenechromium cation exhibits a splitting of the lines due to the interaction with both the central atom (the ^{53}Cr isotope) and with the protons of the benzene rings (Fig. 5): $A_{^{53}Cr}$ = 19 G and A_H = 3.6 G. The substitution of hydrogen atoms by methyl groups does not entail splitting by the CH_3 protons. In the case of the isopropyl and cyclohexyl substituents, a splitting of ~1 G by the α-proton is observed[31]. In the spectrum of the cation $[C_6H_2(CH_3)_4]_2Cr$ the splitting by the ring protons increases to 4.34 G.[41]

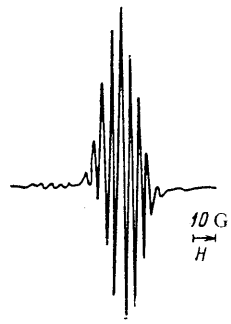


Figure 5. EPR spectrum of the cation $Cr(C_6H_6)_2^+$ in a 1:1 dimethylformamide–chloroform mixture at 200 K.[42]

Analysis of the unpaired electron spin density distribution in the dibenzenechromium cation, assuming delocalisation of the unpaired electron over the π bonds of the ligands, leads to paradoxical results. The employment of the McConnell relation between the splitting A_H and the spin density in the $2p_z$ orbital of the carbon atom ρ_C ($A_H = Q\rho_C$, where Q = −27 G) leads to the conclusion that the overall spin density in the π-electron system of the two benzene rings is approximately equal to two unpaired electrons. On the other hand, the splitting due to the interaction with the ^{53}Cr nucleus in the EPR spectra of inorganic chromium compounds is approximately the same as in the spectrum of the dibenzenechromium cation. This result may be evidence that the unpaired electron in the dibenzenechromium cation is mainly localised at the chromium atom. According to calculations[42], the coefficients α_1, characterising the contribution of the $3d_z$ orbital of the chromium atom to the molecular orbital of the unpaired electron in the dibenzenechromium cation, is close to unity.

Thus the quantitative relations derived on the basis of the study of the π-electron radicals to not hold for the dibenzenechromium cation.

The study of the paramagnetic shifts of the proton signals of the benzene rings and the protons of the methyl groups in the NMR spectra of the dimethyl derivatives of dibenzenechromium cation established the signs of the HFI constants[24,43]. The constant for the splitting by the protons of the benzene ring in the cation $Cr(C_6H_5CH_3)_2^+$ is +3.46 G and that for the splitting by the protons of the methyl groups is −0.46 G.

It has been suggested that the proton HFS is due to the direct interaction of the unpaired electron in the $3d_{z^2}$ orbital with the protons of the benzene ring. Estimates of the contribution of this HFI mechanism showed that it is negligibly small[31,44]. An attempt has been made[24] to explain the observed results by the competition between two mechanisms of the delocalisation of the spin density via π and σ bonds.

As for dinaphthalenevanadium(0), only one naphthalene ring in the dinaphthalenechromium cation is involved in the formation of a bond with the metal. This conclusion is based on the analysis of the proton HFS of the EPR spectrum[35]. The splitting hardly differs from the splittings observed in the spectrum of the dibenzenechromium cation.

4. The EPR and NMR Spectra of Sandwich Compounds of Cobalt

The EPR spectrum of $CoCp_2$ has been investigated at 4 K in a ferrocene single crystal obtained by the joint sublimation of these two compounds[38]. For certain orientations of the crystal, a spectrum with an eight-line HFS, corresponding to the interaction of the unpaired electron with the cobalt nucleus, was recorded. Owing to the uncertainty in the orientation of the crystal, the EPR parameters were not determined accurately: $g_1 = 1.67$, $g_2 = 1.74$, $A = 274$ or 469 MHz, and $B = 274$ or 384 MHz.

More accurate measurements of the EPR parameters of the complex $CoCp_2$ were carried out at 4.2 K in a ruthenocene single crystal: $g_x = 1.140$, $g_y = 1.219$, $g_z = 1.584$, $A_x = +25.5 \times 10^{-4}$ cm^{-1}, $A_y = -120.6 \times 10^{-4}$ cm^{-1}, and $A_z = -103.4 \times 10^{-4}$ cm^{-1}.[42]

Two states have been proposed in accordance with calculations for cobaltocene:

$$(a_{1g}^1)^2(e_{2g})^4(a_{1g}^*)^1 \text{ (Ref.36)}$$

and

$$(a_{1g}^1)^2(e_{2g})^4(e_{2u})^1 \text{ (Ref.3)}$$

The a_{1g}^* orbital is the virtually pure 4s orbital of the metal. In this case the constant for the hyperfine interaction with the cobalt nucleus should be ~4800 MHz,[9] whereas the experimental value is ~300 MHz. The hypothesis that the unpaired electron is located in the non-bonding e_{2u} orbital of the ligand, which does not interact with the cobalt orbital by virtue of symmetry considerations, should lead to a vanishingly weak hyperfine interaction with the cobalt nucleus. The ground state $(e_{2g})^4(a_{1g}^1)^2(e_{1g}^*)^1$ is consistent with the EPR data[38]. It has been shown that spin–orbit coupling, orthorhombic distortion, and the dynamic Jahn–Teller effect influence the EPR parameters of the orbitally degenerate $^2E_{1g}$ ground state of cobaltocene. The e_{1g}^* orbital of the unpaired electron is determined to the extent of 58% by the 3d orbital of the metal and 42% by the π orbital of the ligand.

The contact shift in the ^{1}H NMR spectrum of $CoCp_2$ is +3230 Hz ($\nu_0 = 60$ MHz) and $A_H = -1.01$ G. The ring protons in $Co(C_5H_4CH_3)_2$ are non-equivalent and two lines with shifts of +2917 and 4305 Hz and $A_H = -0.904$ and -1.34 G are observed. The shift of the line of the CH_3 protons is -687 Hz with $A_{CH_3} = 0.214$ G.[9]

The data in Table 8, which presents the contact shifts of the ^{13}C and ^{1}H NMR lines of cobaltocene and its alkyl derivatives, make it possible to follow the characteristics of the spreading of the spin density from the metal atom to the ligand atoms. The signs of the shifts show that the spin density is positive on the carbon atom and negative on the hydrogen atoms of the rings[32].

A large upfield shift of +3535 Hz is observed in the NMR spectrum of the cation $Co(C_6H_6)_2^+$. The substitution by the methyl group in $Co(C_6H_5CH_3)_2^+$ leads to a shift of the line due to the methyl protons by -2650 Hz.[24] The directions and magnitudes of the ring and methyl proton line shifts indicate the predominance of the mechanism involving the delocalisation of the unpaired electron density via the π bonds. The lines of the CH_3 protons in the $Co[C_6(CH_3)_6]_2^+$ spectrum are displaced downfield by 3695 Hz with $A_H = 0.308$ G.

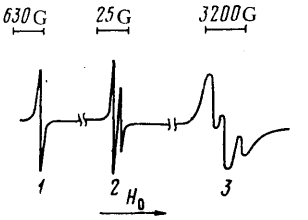


Figure 6. ^{1}H NMR spectrum of the ditoluenecobalt cation in toluene at 298 K: 1) line of the methyl protons of the cation; 2) line of the protons in the solvent molecules; 3) line of the protons in the benzene ring of the cation[24].

When a methyl group is introduced, the lines due to the protons of the benzene rings in the $Co(C_6H_5CH_3)_2^+$ spectrum are split into three signals. Fig.6 shows that the relative intensities of these signals are 2:2:1. These lines have been attributed[24] to the *ortho*- and *meta*-protons (overall intensity 4) and to the proton in the *para*-position (intensity 1). The nature of the splitting of the ring proton lines has been compared with the HFS and the distribution of the unpaired electron density in the toluene radial-anion[46]. Together with the similarity of the spectroscopic data for $Co(C_6H_5CH_3)_2^+$ and $C_6H_5CH_3^-$ (approximate equivalence of the *ortho*- and *meta*-protons and their difference from the *para*-proton), there is also a significant difference, which consists in the fact that the constant for the hyperfine interaction with the proton in the *para*-position in the toluene radical-anion is approximately nine times smaller than the constant for the hyperfine interaction with the protons in the *ortho*- and *meta*-positions. On the other hand, the ratio of these constants in the ^{1}H NMR spectrum of the cation $Co(C_6H_5CH_3)_2^+$ is close to unity. The HFI constant for the protons of the methyl group in the toluene radical-anion is approximately ten times smaller than the HFI constants for the *ortho*- and *meta*-protons. The corresponding quantities for $Co(C_6H_5.CH_3)_2^+$ are of the same order of magnitude and have the same signs, which implies that there is no significant redistribution of the unpaired electron density in the π-electron system of the benzene rings in $Co(C_6H_5CH_3)_2^+$ compared with $Co(C_6H_6)_2^+$.

III. NMR SPECTRA OF NICKELOCENE

McConnell and Holm[47] were the first to observe the proton magnetic resonance of solid nickelocene. The large shift of the NMR proton line which they noted was the first example of the observation of what is nowadays well known as a contact shift.

The EPR spectrum of nickelocene has not been observed in the wavelength range 3.0–0.8 cm and at temperatures from 77 to 4 K.[37] Measurements of the magnetic susceptibility showed that $g_\parallel = 2.0023$, $g_\perp = 2.06$, and the zero-field splitting constant $D = 25.6$ cm^{-1}.[48] Consequently, the magnetic fields and bond lengths used by Nüssbaum and Voitländer[37] were insufficient for the observation of the EPR of nickelocene.

In the ground state of nickelocene $(a_{1g}^1)^2(e_{2g})^4(e_{2u})^2$, proposed on the basis of theoretical calculations, two unpaired electrons are located in the ligand orbital e_{2u}.[3] However,

the large splitting of the signals in a zero field shows that both unpaired electrons are located at the metal atom. It is known that the zero-field splittings or organic triplet molecules are much smaller[49].

The states

$$(a_{1g}^1)^2(e_{2g})^4(e_{1u}^*)$$

and

$$(a_{1g}^1)^2(e_{2g})^4(e_{1g}^*)^2$$

have been proposed for nickelocene on the basis of a study of the magnetic susceptibility[48]. The first state includes the metal $4p_x$ and $4p_y$ orbitals as carriers of the unpaired electron, while in the second the unpaired electron is in the d_{xz} and d_{yz} orbitals. NMR data are consistent with the second state.

Table 8. Paramagnetic shifts (p.p.m.) of the ^{13}C and ^1H NMR lines of cobaltocene, nickelocene, and their alkyl derivatives[32].

Compound	C(1)	C(2, 5)	C(3, 4)	C^α	C^β	H(2, 5)	H(3, 4)	H^β	H^γ
$(C_5H_5)_2Co$	−577	−577	−577	—	—	+56.2	+56.2	—	—
$(CH_3C_5H_4)_2Co$	−358	−437	−755	+112	—	+49.0	+73.6	−12.2	—
$(C_2H_5C_5H_4)_2Co$	−337	−433	−705	+112	−56	—	—	−13.6	−2.4
$(C_4H_9C_5H_4)_2Co$	−458	−458	−633	+94	−123	+50.2	+64.0	—	−2.7
$(C_5H_5)_2Ni$	−1436	−1436	−1436	—	—	+263	+263	—	—
$(CH_3C_5H_4)_2Ni$	−1285	−1475	—	+640	—	+263	+263	−210	—
$(C_2H_5C_5H_4)_2Ni$	—	—	—	+603	−475	+257	+257	−203	−4.5

The study of the ^1H NMR spectra of $NiCp_2$ and $Ni(C_5H_4CH_3)_2$ in solution in toluene at a frequency of 60 MHz and 298 K showed that the ring proton line is displaced by +15300 Hz in the $NiCp_2$ spectrum and by +15190 Hz in the $Ni(C_5H_4CH_3)_2$ spectrum, while the CH_3 proton line is displaced by 11900 Hz. The calculated HFI constants are $A_H = -1.24$ and -1.23 G and $A_{CH_3} = 0.96$ G.[9] Table 8 lists the ^{13}C and ^1H NMR data for nickelocene and its alkyl derivatives. The spin density at the ring carbon atom has the positive sign and that at the ring hydrogen atoms has the negative signs. Comparison of the signs and magnitudes of the contact shifts for the ring and methyl protons shows that the mechanism involving delocalisation via π bonds is most clearly manifested in nickelocene.

IV. EPR SPECTRA OF MANGANOCENE

Depending on the axial splitting (i.e. on the ligand field strength) and on the splitting in a zero magnetic field, the complex $MnCp_2$ can exist in two states: in the high-spin state $(a_{1g}^1e_{2g}^2e_{1g}^2)^6A_{1g}$ and in the low-spin state $(a_{1g}^2e_{2g}^3)^2E_{2g}$ or $(a_{1g}^1e_{2g}^4)^2A_{1g}$. Pure $MnCp_2$ gives rise to a broad EPR signal with $g = 2$, which completely disappears on cooling to 4.2 K.[50]

The environment of $MnCp_2$, which arises on its joint crystallisation with various diamagnetic molecules, has a considerable influence on the form of its EPR spectrum[51]. Manganocene in the $MgCp_2$ lattice exhibits at 4.2 K and a frequency of 9.5 GHz a spectrum characteristic of a high-spin d^5 system with $g \cong 2$, the splitting due to the hyperfine interaction with the ^{55}Mn nucleus being characterised by the constant $A = 65$ G and the order of magnitude of the splitting in a zero magnetic field being equal to the order of magnitude of the applied quantum (0.3 cm^{-1}).

In other isostructural lattices ($FeCp_2$ and $RuCp_2$) manganocene exhibits completely different EPR spectra, which characterises it as a low-spin system. The low-spin $MnCp_2$ state $^2E_{2g}$ is isoelectronic with the state of the ferrocenium cation. As for the ferrocenium cation, a strong anisotropy of the g-factor is observed ($g_\parallel = 3.519$, $g_\perp = 1.222$, $A_\parallel = 52.3 \times 10^{-4}$ cm^{-1}, and $A_\perp = 26 \times 10^{-4}$ cm^{-1} for the $FeCp_2$ lattice)[51]. As in the case of the ferrocenium cation, the introduction of substituents into the cyclopentadienyl ring decreases the anisotropy of the g-factor.

In the $Fe(C_5H_4CH_3)_2$ crystal, the g-factor for the complex $Mn(C_5M_4CH_3)_2$ has the following values: $g_\parallel = 3.06$ and $g_\perp = 1.850$ ($A_\parallel = 11.4 \times 10^{-4}$ cm^{-1} and $A_\perp = 24.5 \times 10^{-4}$ cm^{-1}).[51]

None of the low-spin $MnCp_2$ states gave rise to EPR signals on heating above 77 K. The low-symmetry splitting is $\delta = 200$ cm^{-1} for $MnCp_2$ and $\delta = 630$ cm^{-1} for $Mn(C_5H_4CH_3)_2$. The spin–orbit coupling parameter is $\xi = 260$ cm^{-1}.[51]

The results obtained show that the energies of the low- and high-spin states of manganocene differ by a small amount and weak intermolecular forces are sufficient to alter the ground electronic configurations. The lattices which promote the formation of longer metal–ring bonds favour the appearance of the high-spin system and conversely those promoting the formation of shorter bonds favour the appearance of the low-spin system. The "distance" between these two states is ~0.5 kcal mol^{-1}.[51]

V. THE JAHN–TELLER EFFECT IN SANDWICH COMPOUNDS

In those cases where the orbital state of the ion is degenerate because of symmetry factors, the ligands are acted upon by forces which distort the distribution of the nuclei until the ion assumes a configuration having both a lower symmetry and a lower energy; the existing degeneracy is thereby eliminated (the Jahn–Teller effect). The theory of the Jahn–Teller effect and its manifestation in the EPR spectra of coordination compounds have been described in monographs[52,53].

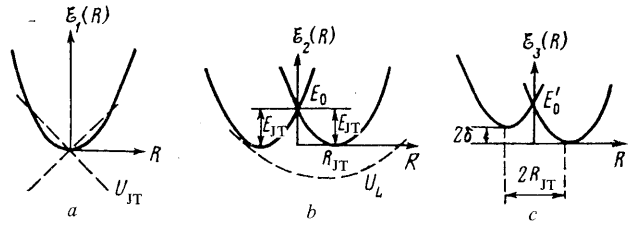


Figure 7. Schematic representation of sections through potential surfaces: *a*) for an orbitally non-degenerate complex; *b*) and *c*) section along the active Jahn–Teller coordinate of a doubly orbitally degenerate complex.

The electronic rearrangements arising as a result of the Jahn–Teller effect can be accounted for qualitatively by considering the potential energy surfaces (Fig.7). In contrast to the orbitally non-degenerate complexes [$\mathscr{E}_1(R)$, Fig.7*a*], in an orbitally degenerate complex there are several equivalent potential energy minima stabilised by the energy associated with the Jahn–Teller effect (E_{JT}) and displaced by an amount R_{JT} relative to the nuclear configuration corresponding to the maximum symmetry of the complex [$\mathscr{E}_2(R)$, Fig.7*b*]. The curves in Fig.7*b* have been obtained from the plot illustrated in Fig.7*a* by adding to the $\mathscr{E}_1(R)$ potential energy curve the linear potential U_{JT} with the opposite slope.

The superposition of the weak asymmetric perturbing potential U_L (for example, the field of the surrounding molecules) onto the symmetrical potential $\mathscr{E}_2(R)$ leads to the appearance of an asymmetric potential $\mathscr{E}_3(R)$ (Fig.7c).

Potential surfaces known as the "sombrero" or "Mexican hat" surfaces correspond to octahedral complexes whose symmetry has been distorted by the Jahn–Teller effect. The shape of the surface is determined by the interaction of the doubly degenerate electronic E level with the doubly degenerate e vibration. Such a surface is obtained by rotating the potential energy curve illustrated in Fig.7b about the ordinate axis. The geometrical locus of the points orresponding to the energy minimum is a circumference with the radius R_{JT}.[53] Allowance for the quadratic terms in the Jahn–Teller potential leads to an increase in the complexity of the form of the potential surface and to the appearance of three minima on the above circumference, corresponding to distortions of the octahedra along three different axes. Fig.8 illustrates an expanded section through the lower surface for the E level of the octahedral complex; both the energy of the vibrational quantum $\hbar\omega$ and the tunnel splitting Δ, determining the probability of the transition between the minima, are shown. The manifestation of the Jahn–Teller effect in the EPR spectra depends on the ratios of E_{JT}, $\hbar\omega$, and Δ.

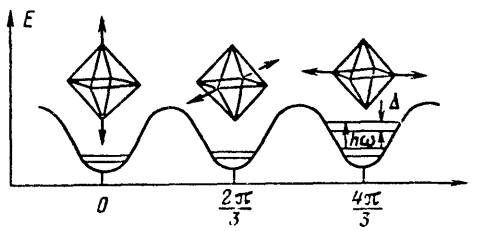


Figure 8. Potential surface corresponding to the distortions of an octahedral complex along three axes: $\hbar\omega$ = energy of vibrational quantum; Δ = tunnel splitting.

Numerous data on the manifestation of the Jahn–Teller effect in the EPR spectra have been obtained for crystals containing the Cu^{2+} ion. The characteristic features of this manifestation are as follows. At high temperatures the spectrum is characterised by an isotropic g-factor of ~2.2. As the temperature is reduced, the form of the spectrum changes reversibly with temperature in a certain transition region. The temperature range in which this occurs is different for different salts and is usually below 60 K, most frequently in the range from 40 to 4 K. At temperatures below the transition region three different spectra with anisotropic g-factors ($g_\parallel \cong 2.4$, $g_\perp \cong 2.1$) are observed; these spectra have axial symmetry relative to each of three mutually perpendicular fourfold axes of the complex CuY_6. A characteristic feature of the behaviour of the spectrum in the transition region is the simultaneous existence of anisotropic and isotropic spectra. With increase of temperature, the intensity of the lines of the first spectrum falls and that of the second increases.

Within the framework of the qualitative description of the Jahn–Teller effect presented above, the temperature-induced changes in the spectra of CuY_6 are described as follows. If $E_{JT} > \hbar\omega$ and the temperature is below the transition region, then the distortion of the octahedron is stable. The system is in one of the minima. Since an increase in the length of one of the three axes of the octahedron takes place at random, the observation of three anisotropic spectra corresponds to their random orientation relative to the direction of the magnetic field. An increase of temperature leads to the population of the excited vibrational states. Whereas the tunnel splitting is small in the zeroth vibrational level, in the excited states it increases sharply, as a result of which the distortion of the complex ceases to be stable and begins to move along its axes. If the quantity $\gamma_e(g_\parallel - g_\perp)\mu_0 H$ (γ_e is the gyromagnetic ratio of the electron) is smaller than $1/\tau$ (the rate of transition between equivalent distortions), then one line corresponding to $\bar{g} = 1/3(g_\parallel + 2g_\perp)$ will be recorded in the spectrum. On the other hand, if $E_{JT} < \hbar\omega$, the distortion is unstable within the limits of a single minimum however low the temperature. The Jahn–Teller effect influences not only the form of the EPR spectrum but also the g-factors and the HFI constants.

The influence of the Jahn–Teller effect on the low-spin d^5 and d^7 states of metallocenes has been investigated in studies[54,55] dealing with cobaltocene, manganocene, ferrocenium cations, and nickelocenium cations. Paramagnetic complexes have been investigated in a large number of different diamagnetic crystal lattices in order to estimate the influence of the asymmetric environment on the parameters of the spin-Hamiltonian. For all the orbitally degenerate d^5 and d^7 complexes, an appreciable dependence of the g-tensor on the structure of the crystal lattice has been observed. On the other hand, the absence of the sensitivity by the magnetic parameters to the molecular environment is characteristic of orbitally non-degenerate complexes [vanadocene, $d^3(^4A_{1g})$].

When the Jahn–Teller effect is taken into account, the g-factor is found to depend on the selected orbital moment quenching factor V in addition to its dependence on the low-symmetry distortion δ. The formula quoted above assumes the following form for g_z of the ferrocenium cation with allowance for V: $g_z = 2 + 4KXV/(1 + X^2)^{1/2}$. In the absence of the Jahn–Teller effect, $V = 1$, tending to zero in the case of a strong linear Jahn–Teller effect. For the separate determination of KV and $X = -\zeta/\delta$, Ammeter and coworkers[54,55] used terms of the spin-Hamiltonian other than g_z. The determination of the factor V as a function of the parameter δ in various crystal lattices showed that the dynamic Jahn–Teller motion of a free molecule is suppressed by the increasing asymmetric fields of the matrix. Systematic variation of the lattice structure and the introduction of substituents into the cyclopentadienyl ring made it possible to observe a gradual transition from the purely dynamic Jahn–Teller effect to the limiting case of a static distortion of the complexes. Extrapolation to the case of a free molecule ($\delta = 0$) shows that, for all the orbitally degenerate systems investigated, the distortion of the C_5H_5 rings remains fully dynamic, i.e. the Jahn–Teller stabilisation energy E_{JT} does not exceed the energy of the quantum $\hbar\omega$ corresponding to the active vibration. Ammeter and coworkers[54,55] considered different types of vibrations and indicated those which are active as regards the formation of a linkage between the electronic and vibrational motions.

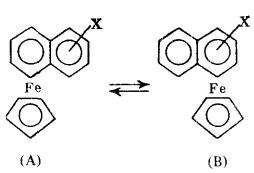
There are indications of the possibility of the existence also of the static Jahn–Teller effect in metallocenes. X-Ray diffraction analysis of decamethylferrocene [$d^6(^1A_{1g})$] and decamethylmanganocene [$d^5(^2E_{2g})$] revealed a distortion of the symmetry for the orbitally degenerate manganocene complex[56].

A pattern analogous to that observed in the case of Cu^{2+} ions has been observed in the study of the EPR spectra of naphthalenecyclopentadienyliron[57]. The anisotropic signal at 77 K ($g_\parallel = 2.09$, $g_\perp = 2.006$) is converted into an isotropic signal at 150 K with $\bar{g} = 1/3(g_\parallel + 2g_\perp)$. Averaging of the anisotropy of the g-factor with increase of temperature has

also been observed for other arenecyclopentadienyliron complexes near the melting point of 1,2-dimethoxyethane (−70 °C), in which these complexes have been obtained by reducing the corresponding cations with sodium[25].

The possibility of the manifestation of the Jahn–Teller effect in arenecyclopentadienyliron complexes is determined by the quasi-degenerate nature of the iron states $d^7(^2E_{1g})$, split owing to the low-symmetry interaction with the arene ligand. A characteristic feature of the chemical bond in the given compounds compared with the dicyclopentadienyl compounds consists in the fact that the symmetries of the molecular wave functions of the arene and cyclopentadienyl ligands are different. For this reason, the common molecular orbitals leading to the formation of a chemical bond are formed only from the fully symmetrical molecular orbitals of the ligands. Other (higher) occupied orbitals consist only of combinations of the atomic orbitals of the iron atom with the molecular orbitals of the cyclopentadienyl ring[58]. In the fully symmetric molecular wave function of naphthalene, the maximum electron density corresponds to the 9- and 10-positions and one can assume that an energy minimum in the neutral complex corresponds to the symmetrical position of the iron atom when no account is taken of the Jahn–Teller effect. The distortion of this symmetrical structure associated with the shift of the iron atom towards the centre of one of the benzene rings of naphthalene can lead to the appearance of two potential energy minima located symmetrically relative to the bond between the carbon atoms in the 9- and 10-positions. The tunnelling of the iron atom between these two minima in combination with the rotation of the naphthalene ligand about the bond between naphthalene and the iron atom should lead to the averaging of the anisotropy of the g-factor.

In order to confirm the above model of motion, the EPR spectra of α-$CH_3C_{10}H_7FeC_5H_5$ and β-$FC_{10}H_7FeC_5H_5$ were obtained[57]. At 77 K their spectra do not differ from that of $C_{10}H_8FeC_5H_5$. With increase of temperature, the $g_\parallel$ signals in the spectra of α-$CH_3C_{10}H_7FeC_5H_5$ and β-$FC_{10}H_7FeC_5H_5$ are split into two components. The appearance of two $g_\parallel$ signals was attributed to the existence of two isomers (A) and (B):



(A) (B)

At 77 K only the single isomer (A) exists, being the most stable, while with increase of temperature the isomer (B) also arises as a result of the migration of the iron atom. The quantity $g_\parallel^A - g_\parallel^B$ corresponds to the energy difference $\Delta E_{AB} \cong 200$ cm^{-1}. The energy of the vibrational quantum (300 cm^{-1}) and the tunnel splitting (1 − 3 cm^{-1}) were determined from the temperature variation of the EPR spectrum of $C_{10}H_8FeC_5H_5$.[57]

VI. THE ELECTRONIC STRUCTURE OF METALLOCENES AND THE MECHANISM OF SPIN DELOCALISATION

In combination with electronic absorption spectroscopic, photoelectron spectroscopic, and γ-spectroscopic data as well as the results of quantum-chemical calculations, the magnetic resonance data presented make it possible to describe fairly completely the entire scheme of the energy levels of metallocenes and fit qualitatively quite well within the general sequence of the energy levels of metallocenes: $a_{1g} \leqslant e_{2g} \ll e_{1g}^*$. A quantitative description of the above scheme based on experimental data is impossible in the absence of theoretical analysis.

The d–d transition bands in the electronic absorption spectra of the d^6 metallocenes $Fe(C_5H_5)_2$, $Ru(C_5H_5)_2$, and $Co(C_5H_5)_2^+$ were analysed within the framework of the ligand field theory[59]. The following one-electron parameters characterising the energy level scheme were obtained: $\Delta_1 = \varepsilon(e_{2g}) - \varepsilon(a_{1g}) = 7000$ cm^{-1} and $\Delta_2 = \varepsilon(e_{1g}^*) - \varepsilon(a_{1g}) \cong 22000 - 30000$ cm^{-1}. The result $e_{2g} < a_{1g}$ conflicts with the EPR data for ferrocenium, the ground state of which is $^2E_{2g}$. According to non-empirical calculations for ferrocene, $e_{2g} > a_{1g}$.[60] Within the framework of non-empirical calculations for ferrocene, considerable differences (10000 cm^{-1}) arise on comparing the energies of the d–d transition bands with the differences between the total energies of the ground and excited states and the difference between the energies of the "frozen" molecular orbitals. Although the first method is more rigorous, it is difficult to give preference to it from the standpoint of agreement with experiment[60]. In the theoretical analysis of the ionisation potentials, the above differences reach approximately 6 eV, which makes it necessary to treat with caution the estimate of the distance between different orbitals from the difference between the ionisation potentials (the Koopmans theorem). The principal source of the large differences is the contribution of the electronic relaxation and of the energy of the rearrangement of the electron cloud on ionisation of the complex[61].

Analysis of the charge-transfer bands makes it possible to estimate the distance from the energy levels of the metal to the levels of the ligand[59,60]. The bands of the d–d transitions between the a_{1g}, e_{2g}, and e_{1g}^* orbitals and the charge-transfer bands are in the visible and ultraviolet regions. According to the available data, the possible transitions between the a_{1g} and e_{2g} orbitals occur in the red and infrared regions. One of the infrared bands (200 cm^{-1}) in the ferrocenium spectrum has been assigned to the electronic transition between the $^2E_2$ and $^2A_1$ states[62].

Thus the fundamental energy level scheme for sandwich compounds has now been firmly established and is quite fully characterised in quantitative terms. A compilation of the electronic states of certain complexes, based on the analysis of theoretical and experimental data, has been published[24] (Table 9).

Table 9. The electronic configurations of various metallocenes and diarene complexes.

Complex	No. of d electrons	Electronic configuration	Ground state
$V(Cp)_2$	3	$(e_{2g})^2(a_{1g})^1$	$^4A_{1g}$
$Cr(Cp)_2$	4	$(e_{2g})^3(a_{1g})^1$	$^3E_{2g}$
$V(C_6H_6)_2^+$	4	$(e_{2g})^3(a_{1g})^1$	$^3E_{2g}$
$Cr(C_6H_6)_2^+$	5	$(e_{2g})^4(a_{1g})^1$	$^2A_{1g}$
$Fe(Cp)_2^+$	5	$(a_{1g})^2(2_{2g})^3$	$^2E_{2g}$
$V(C_6H_6)_2$	5	$(e_{2g})^4(a_{1g})^1$	$^2A_{1g}$
$Cr(C_6H_6)_2$	6	$(e_{2g})^4(a_{1g})^2$	$^1A_{1g}$
$Fe(Cp)_2$	6	$(e_{2g})^4(a_{1g})^2$	$^1A_{1g}$
$Fe(C_6(CH_3)_6)_2^+$	6	$(e_{2g})^4(a_{1g})^2$	$^1A_{1g}$
$Co(Cp)_2$	7	$(e_{2g})^4(a_{1g})^2(e_{1g})^1$	$^2E_{1g}$
$Fe(C_6(CH_3)_6)_2^+$	7	$(e_{2g})^4(a_{1g})^2(e_{1g})^1$	$^2E_{1g}$
$Ni(Cp)_2$	8	$(e_{2g})^4(a_{1g})^2(e_{1g})^2$	$^3A_{1g}$
$Co(C_6(CH_3)_6)_2^+$	8	$(e_{2g})^4(a_{1g})^2(e_{1g})^2$	$^3A_{1g}$
$Ni(C_6(CH_3)_6)_2^+$	8	$(e_{2g})^4(a_{1g})^2(e_{1g})^2$	$^3A_{1g}$

The most complex problem in the description of the electronic structure of the compounds considered here is the mechanism of the delocalisation of spin density. The attempts undertaken hitherto at the calculation of the distribution of spin density cannot be regarded as satisfactory,

because they were based solely on the idea of the competition between processes involving delocalisation via the π and σ bonds[63]. ^{13}C NMR data for metallocenes showed that the delocalisation pattern is more complex. It is seen from a comparison of the ^{13}C NMR spectra of various metallocenes that, depending on the nature of the metal, not only the magnitude but also the sign of the paramagnetic shift changes. Whereas the shift is negative for nickelocene and cobaltocene, it is positive for vanadocene and chromocene, which corresponds to a negative spin density of the unpaired electron on the carbon atom. Although the signs of the shifts of the proton signals of metallocenes are correlated with the signs of the shifts of the ^{13}C nuclei in accordance with the McConnell equation, a quantitative correspondence is not observed.

In order to account for the magnitude of the ^{13}C shifts, it was suggested that one assumes that they are determined by the sum of three contributions[64]:

$$\sigma^{c}_{obsd} = \sigma^{\pi}_{con} + \sigma^{\sigma}_{con} + \sigma_{dip} ,$$

where the σ^{π}_{con} contribution is of a complex type. It can include directly the unpaired electron density due to the exchange interaction between the 3*d* orbitals of the metal and the $2p_z$ orbitals of the ligands. This situation apparently arises in nickelocene and cobaltocene. However, the spin density can be displaced onto the carbon atoms also via a different pathway resulting from an indirect polarisation mechanism. The polarisation mechanism operates in those cases where the degree of direct conjugation is slight or zero. According to the theory[65], the interaction of the unpaired electron with the electrons in the occupied orbitals results in the motion of electrons with α- and β-spins in somewhat different orbitals. The summation of the spin densities over all the occupied orbitals results in the possibility of the appearance of a spin density at an individual atom with both positive and negative signs. It is believed[64] that the polarisation of the atomic orbitals of the metal and their interaction with the π orbitals of the ligands leads to the appearance of a negative spin density on the carbon atoms in vanadocene and chromocene.

Although the exchange polarisation does predominate in the transfer of spin density to the carbon atoms of vanadocene and chromocene, the available data show that there is a simultaneous direct delocalisation of the positive spin density via the σ orbitals, which leads to a negative contribution to the shift of the ^{13}C NMR lines. This effect is manifested by a smaller ratio of the shifts of the ^{13}C and ^{1}H lines, which is −2 for vanadium compared with −4.5 for nickel[64].

Direct exchange between the 3*d* electrons of the metal and the σ orbitals located in the plane of the cyclopentadienyl rings should lead to higher HFI constants as a consequence of the significant *s* character of these orbitals. The pseudo-contact contribution is apparently small for vanadocene and chromocene, since they are in the *A* states and the degree of anisotropy of their *g*-factors is small. However, this contribution can be appreciable for chromocene and cobaltocene.

The separation of the contributions determining the HFI constants and the contact shifts of the ^{13}C and ^{1}H lines is important for the understanding of the nature of the aromaticity and the properties of the π-electron system of the complexes investigated, particularly in the case of substituted metallocenes and diarene complexes. The results exhibit significant differences between the properties of the free ligands and the ligands in the complexes.

Measurements were made of the paramagnetic shifts in the ^{13}C and ^{1}H NMR spectra of symmetrical polymethyl-substituted ferrocenium cations. The isolation of the contact (Fermi) and pseudo-contact (dipole–dipole) terms showed that the signs of the contact shifts for the carbon atoms of the cyclopentadienyl rings vary in a complex manner as a function of the number and positions of the methyl groups[66,67]. When one methyl group is introduced, the sign of the contact shift changes from negative to positive only at the carbon atom linked to the CH_3 group. When four methyl groups are introduced, the contact shifts at all the carbon atoms, with the exception of the unsubstituted atom, acquire positive signs. If the number of methyl groups in the cyclopentadienyl ring is 0, 2, 3, and 5, then a negative contact shift is characteristic of all the carbon atoms in the ring. In order to explain the complex distribution of spin density, it proved necessary to take into account, apart from the competition between different delocalisation mechanisms mentioned above, the thermal population of the close vacant *d* orbitals by the unpaired electron and the influence of the splitting of the degenerate levels of the molecular π orbitals of cyclopentadienyl under the influence of substituents.

---o0o---

The analysis of the experimental and theoretical studies on sandwich compounds indicates a considerable progress in the understanding of the nature of the complex organometallic chemical bond. The many-electron nature of this bond determines the existence of a large number of interesting effects, vigorous investigation of which is being continued.

REFERENCES

1. H.H.Jaffé, J.Chem.Phys., 1953, **21**, 156.
2. E.M.Shustorovich and M.E.Dyatkina, Dokl.Akad.Nauk SSSR, 1959, **128**, 1234; 1960, **133**, 141.
3. J.P.Dahl and C.J.Balhausen, Kgl.Danske Viedenskab., Selskab, Mat.fys.Medd., 1961, **33**, 5.
4. C.J.Ballhausen, "Introduction to Ligand Field Theory", McGraw Hill, New York, 1962, p.218.
5. M.Yamazaki, J.Chem.Phys., 1955, 23, 1260.
6. W.Moffitt, J.Amer.Chem.Soc., 1954, **76**, 3386.
7. M.Risenblum, "Chemistry of the iron Group Metallocenes", Intersci.Publ., New York, 1965.
8. R.E.Robertson and H.M.McConnell, J.Phys.Chem., 1960, **64**, 70.
9. M.F.Rettig and R.S.Drago, J.Amer.Chem.Soc., 1969, **91**, 1361.
10. J.P.Jesson, J.Chem.Phys., 1967, **47**, 579.
11. R.Prins and F.J.Reinders, J.Amer.Chem.Soc., 1969, **91**, 4929.
12. R.Prins and A.R.Korswagen, J.Organometal.Chem., 1970, 25, C-74.
13. D.A.Levy and L.E.Orgel, Mol.Phys., 1961, **4**, 93.
14. D.K.Scott and R.S.Becker, J.Organometal.Chem., 1965, **4**, 409.
15. R.Prins, Mol.Phys., 1970, **19**, 603.
16. A.Horsfield and A.Wassermann, J.Chem.Soc.A, 1970, 3202.
17. A.Horsfield and A.Wassermann, J.Chem.Soc., Dalton Trans., 1972, 187.
18. R.Prins and A.G.Korbeck, J.Organometal.Chem., 1971, **33**, C-33.
19. H.P.Fritz, H.J.Keller, and K.E.Schwarzhans, J.Organometal.Chem., 1966, **6**, 632.
20. S.E.Anderson and R.Rai, Chem.Phys., 1972, **2**, 216.
21. F.H.Köhler, J.Organometal.Chem., 1974, **69**, 145.
22. F.H.Köhler, J.Organometal.Chem., 1974, **64**, C-27.
23. H.Brintziger, G.Palmer, and R.H.Sands, J.Amer. Chem.Soc., 1966, **88**, 623.
24. S.E.Anderson and R.S.Drago, J.Amer.Chem.Soc., 1970, **92**, 4244.

25. S.P.Solodovnikov, A.N.Nesmeyanov, N.A.Volkenau, and L.S.Kotova, J.Organometal.Chem., 1979, **182**, 239.
26. S.P.Solodovnikov, A.N.Nesmeyanov, N.A.Volkenau, and L.S.Kotova, J.Organometal.Chem., 1980, **201**, C-45.
27. R.G.Sutherland, S.C.Chen, W.J.Pannekoek, and C.C.Lee, J.Organometal.Chem., 1971, **117**, 61.
28. H.H.Dearman, W.W.Porterfield, and H.M.McConnell, J.Chem.Phys., 1961, **34**, 696.
29. H.M.McConnell, W.W.Porterfield, and R.E.Robertson, J.Chem.Phys., 1959, **30**, 442.
30. R.Prins, P.Bilben, and J.D.Van Voorst, J.Chem. Phys., 1967, **46**, 1216.
31. S.I.Vetchinkin, S.P.Solodovnikov, and V.M.Chibrikin, Optika i Spektrosk., 1960, **8**, 137.
32. F.H.Köhler, J.Organometal.Chem., 1976, **110**, 235.
33. K.H.Hausser, Z.Naturforsch., 1961, **16a**, 1190.
34. G.Henrici-Olivé and S.Olivé, Z,phys.Chem.(Frankfurt), 1967, **56**, 223.
35. C.Henrici-Olivé and S.Olivé, J.Amer.Chem.Soc., 1970, **92**, 4831.
36. E.M.Shustorovich and M.E.Dyatkina, Zhur.Neorg. Khim., 1961, **6**, 249 [Russ.J.Inorg.Chem., 1961(1)].
37. M.Nüssbaum and J.Voitländer, Z.Naturforsch., 1965, **20a**, 1411.
38. M.Nüssbaum and J.Voitländer, Z.Naturforsch., 1965, **20a**, 1417.
39. E.M.Shustorovich and M.E.Dyatkina, Dokl.Akad.Nauk SSSR, 1960, **131**, 113.
40. R.D.Peltham, P.Sogo, and M.Calvin, J.Chem.Phys., 1954, **26**, 1354.
41. B.G.Gribov, B.I.Kozyrkin, A.D.Krivospitskii, and G.K.Chirkin, Dokl.Akad.Nauk SSSR, 1970, **193**, 91.
42. R.Prins and F.Reinders, J.Chem.Phys.Letters, 1969, **3**, 45.
43. Y.U.Karimov, V.M.Chibrikin, and I.F.Shchegolev, J.Phys.Chem.Solids, 1963, **24**, 1683.
44. S.E.Anderson and R.S.Drago, J.Amer.Chem.Soc., 1969, **91**, 3656.
45. J.H.Ammeter and J.D.Swalen, J.Chem.Phys., 1972, **57**, 683.
46. S.P.Solodovnikov, Zhur.Strukt.Khim., 1961, **2**, 282.
47. H.M.McConnell and C.H.Holm, J.Chem.Phys., 1957, **27**, 314.
48. R.Prins and J.D.Van Voorst, Chem.Phys.Letters, 1967, **1**, 54.
49. J.E.Wertz and J.R.Bolton, "Electron Spin Resonance: Elementary Theory and Practical Applications" (Translated into Russian), Izd.Mir, Moscow, 1975, p.238.
50. J.Voitländer and E.Schimitschek, Z.Elektrochem., 1957, **61**, 941.
51. J.H.Ammeter, R.Bucher, and N.Osvald, J.Amer. Chem.Soc., 1974, **96**, 7833.
52. A.Abragam and B.Bleaney, "Electron Paramagnetic Resonance of Transition Metal Ions" (Translated into Russian), Izd.Mir, Moscow, 1972, Vol.1, p.505; 1973, Vol.2, p.238.
53. I.B.Bersuker, "Elektronnoe Stroenie i Svoistva Koordinatsionnykh Soedinenii" (Electronic Structure and Properties of Coordination Compounds), Izd. Khimiya, Moscow, 1976, p.192.
54. J.H.Ammeter, J.Magn.Res., 1978, **30**, 299.
55. J.H.Ammeter, N.Oswald, and R.Bucher, Helv.Chim. Acta, 1975, **58**, 671.
56. D.P.Freyberg, J.L.Robbins, K.N.Raymond, and J.C.Smart, J.Amer.Chem.Soc., 1979, **101**, 892.
57. S.P.Solodovnikov, A.N.Nesmeyanov, N.A.Volkenau, and L.S.Kotova, J.Organometal.Chem., 1980, 201, 447.
58. D.W.Clack and K.D.Warren, J.Organometal.Chem., 1978, **152**, C-60.
59. Y.S.Sohn, D.N.Hendrickson, and N.B.Grey, J.Amer. Chem.Soc., 1971, **93**, 3603.
60. M.M.Rohmer, A.Veillard, and M.H.Wood, Chem.Phys. Letters, 1974, **29**, 466.
61. P.S.Bagus, U.I.Walgren, and J.Almlof, J.Chem.Phys., 1975, **62**, 4628.
62. B.F.Gächter, I.A.Königstein, and V.T.Aleksanjan, J.Chem.Phys., 1975, **62**, 4628.
63. M.F.Retig and R.S.Drago, J.Amer.Chem.Soc., 1969, **91**, 3432.
64. S.E.Anderson and N.A.Matwiyoff, Chem.Phys. Letters, 1972, **13**, 150.
65. A.D.McLachlan, Mol.Phys., 1960, 3, 233.
66. I.R.Lyatifov, S.P.Solodovnikov, V.N.Babin, and R.B.Materikova, Z.Naturforsch., 1979, **34b**, 863.
67. R.B.Materikova, V.N.Babin, S.P.Solodovnikov, I.R.Lyatifov, P.V.Petrovsky, and E.I.Fedin, Z.Naturforsch., 1980, **35b**, 1415.

Nesmeyanov Institute of Organoelemental Compounds, USSR Academy of Sciences, Moscow